

BBAPRO 33887

Oxidative decarboxylation of 3,4-dihydroxymandelic acid to 3,4-dihydroxybenzaldehyde: electrochemical and HPLC analysis of the reaction mechanism

Thomas H. Czaplá^{1,*}, M. Roger Claeys^{2,*}, Thomas D. Morgan³, Karl J. Kramer³,
Theodore L. Hopkins¹ and M. Dale Hawley²

¹ Department of Entomology, Kansas State University, Manhattan, KS, ² Department of Chemistry, Kansas State University, Manhattan, KS and ³ U.S. Grain Marketing Research Laboratory, ARS-USDA, Manhattan, KS (U.S.A.)

(Received 19 September 1990)

Key words: 3,4-Dihydroxymandelic acid; Oxidative decarboxylation; *p*-Benzoquinone methide; Electrochemical oxidation; 3,4-Dihydroxybenzaldehyde; *o*-Benzoquinone

Cyclic voltammetric and chronoamperometric data are consistent with a process in which 3,4-dihydroxymandelic acid (DOMA) is oxidized initially in a two-electron step to its corresponding *o*-benzoquinone. This species is unstable and undergoes the rate-determining loss of CO₂ ($k = 1.6 \text{ s}^{-1}$ at pH 6 and 25 °C) to give an unobserved *p*-benzoquinone methide intermediate that rapidly isomerizes to 3,4-dihydroxybenzaldehyde (DOBAL), DOBAL is also electroactive at the applied potential and is oxidized in a two-electron step to 4-formyl-1,2-benzoquinone. Subsequent reactions of 4-formyl-1,2-benzoquinone include the oxidation of unreacted DOMA and the hydration of its aldehyde functional group. Oxidation of DOMA directly to its *p*-benzoquinone methide apparently does not occur. Derivatives of mandelic acid (e.g., 4-hydroxymandelic acid) that are expected to give only their corresponding *p*-benzoquinone methides upon oxidation afford redox behavior that differs distinctly from that for DOMA.

Introduction

Oxidation of the *o*-diphenolic moiety of catecholamines and related alcohols, aldehydes and acids to quinones occurs in biological processes, such as arthropod cuticle sclerotization, melanin biosynthesis and plant tissue browning and lignification [1,2]. These reactions are catalyzed by oxidases, such as the tyrosinases, laccases and peroxidases. The former enzymes are copper oxidases with broad substrate specificity that generate *o*-benzoquinone products from a wide variety of *o*-diphenols [3,4]. In addition, other activities ascribed to tyrosinase include the *o*-hydroxylation of monophenols and aromatic amines, oxidation of *o*-aminophenols and *o*-dihydroxyindoles and oxidative decarboxylation of

3,4-dihydroxymandelic acid (DOMA) [3]. DOMA has been reported to be an oxidation product of norepinephrine in cockroaches and may be an intermediate in the synthesis of 3,4-dihydroxybenzaldehyde (DOBAL) and 3,4-dihydroxybenzoic acid, which are precursors of sclerotization agents in cockroach egg cases [5,6].

On the basis of spectroscopic data and product analysis, Sugumaran and co-workers [7,8] reported that tyrosinase catalyzes the oxidative decarboxylation of DOMA and proposed that the corresponding *p*-benzoquinone methide is formed directly instead of the more conventional *o*-benzoquinone derivative. In contrast, Ortiz et al. [9], Cabanes et al. [10] and Bouheroum et al. [11] have presented spectroscopic, kinetic and electrochemical data supporting the hypothesis that only the *o*-benzoquinone of DOMA is generated enzymatically and that the decarboxylation step, which produces a transient *p*-benzoquinone methide intermediate, is a spontaneous chemical reaction not catalyzed by tyrosinase.

We have also studied the oxidation of DOMA and related compounds using cyclic voltammetry, single-potential-step chronoamperometry, controlled-potential coulometry and HPLC [12]. The general goals of our work were to detect and identify the intermediates and

* Present addresses: T.H.C., Department of Biotechnology Research, Pioneer Hi-Bred International, Johnston, IA and M.R.C., BASF Wyandotte, Freeport, TX (U.S.A.).

Abbreviations: DOMA, 3,4-dihydroxymandelic acid; DOBAL, 3,4-dihydroxybenzaldehyde; HPLC, high-performance liquid chromatography; ECE, electron transfer, chemical reaction, electron transfer.

Correspondence: M.D. Hawley, Department of Chemistry, Kansas State University, Manhattan, KS 66506-3701, U.S.A.

the principal products arising from the electrochemical oxidation of DOMA and to study the kinetics of the decarboxylation reaction. A specific goal was to ascertain whether or not the electrochemical oxidation of DOMA leads directly or indirectly to the corresponding *p*-benzoquinone methide.

Materials and Methods

Electrochemical instrumentation and procedures

The cyclic voltammetric and chronoamperometric experiments were performed using a three-electrode potentiostat that incorporated circuits for the electronic correction of ohmic potential loss between the reference and working electrodes. Control of both the potentiostat and the function generator and data acquisition were performed with a laboratory digital computer (ADAC Model 2000, LSI 11/2).

Cyclic voltammetric and chronoamperometric experiments were performed with a renewable carbon paste working electrode (0.5 cm diameter), a saturated calomel reference electrode (SCE) and a platinum flag auxiliary electrode. In order to minimize potentially adverse effects of film formation, the carbon paste electrode surface was renewed between runs. The solution was purged of oxygen with a stream of nitrogen gas for a minimum of 5 min prior to each series of experiments and for approx. 1 min after each removal from and reinsertion into the electrolysis solution of the carbon paste electrode.

The anode material for controlled potential electrolyses was reticulated vitreous carbon (Electro Synthesis; 39 pores per linear cm; 5 cm × 5 cm × 1.25 cm). The electrical conductor to the anode was a platinum wire that was attached to the reticulated vitreous carbon by means of silver epoxy cement. The anode compartment was separated from the saturated calomel reference electrode and the platinum auxiliary electrode by means of a glass frit. Mass transfer was effected by both a stream of nitrogen gas and magnetic bar stirring.

Chemicals, solutions and product analysis

All organic compounds were commercially available and were used as received. Buffers were prepared by adjusting 0.1 M solutions of H₃PO₄ or KH₂PO₄ to the desired pH with 1 M NaOH. Electrochemical oxidation products either were directly injected into a chromatograph or were adsorbed onto alumina and the *o*-diphenols recovered in 1 M acetic acid prior to injection. The primary mobile phase for liquid chromatography consisted of methanol (10%, v/v) and pH 3 phosphate buffer (0.1 M). A second mobile phase consisted of methanol (11% v/v), 0.12 mM sodium octyl sulfate, 0.06 mM disodium EDTA and pH 3.5 phosphate buffer

(0.1 M). A C-18 column was employed with a mobile phase flow rate of 1 ml/min. Products were detected with either a Kratos Analytical Spectraflow 757 absorbance detector set at 280 nm or a Bioanalytical Systems LC-4B electrochemical detector operated at 720 mV. Reaction products were identified by comparing the retention times of unknown compounds with standard compounds from the mandelic acid or benzaldehyde series using two different mobile phases. Identifications were also based on previous spectrophotometric, electrochemical and HPLC evidence for the same or similar reactants [9–11].

Results and Discussion

Cyclic voltammetric behavior of DOMA (I)

The cyclic voltammetric behavior of DOMA was examined as functions of scan rate ($0.1 \text{ V/s} \leq v \leq 100 \text{ V/s}$) and pH ($1 \leq \text{pH} \leq 8$). The interpretations of the cyclic voltammograms were not straightforward because of the effects of slow heterogeneous electron transfer at the carbon paste working electrode, the occurrence of homogeneous chemical reactions with all electrogenerated *o*-benzoquinone intermediates and the overlapping of cyclic voltammetric peaks for the reactants and several of the products.

At pH 2 and a scan rate of 20 V/s, the principal processes on the first cyclic voltammetric cycle consist of an anodic peak near 1.3 V and a cathodic peak near -0.3 V (Fig. 1a). Although the separation of 1.6 V between the anodic and cathodic peaks greatly exceeds

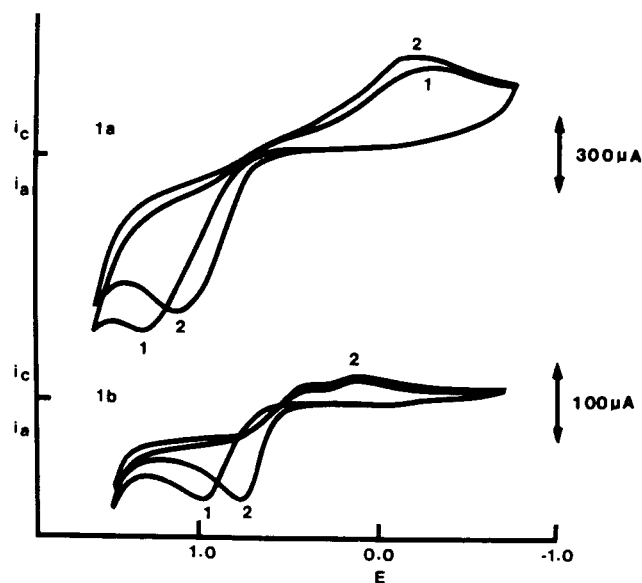
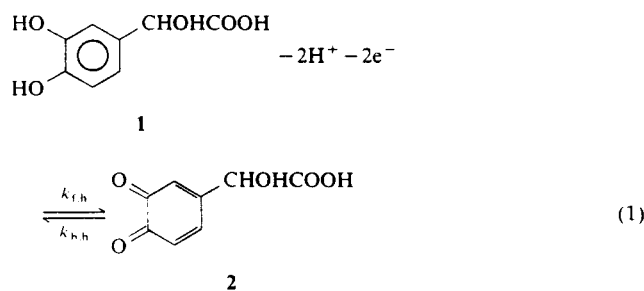


Fig. 1. Cyclic voltammograms of DOMA on a carbon paste electrode surface at pH 2 and 23°C. The numbers 1 and 2 represent the first and second cycles, respectively. (a) Scan rate = 20 V/s; [DOMA] = 0.92 mM. (b) Scan rate = 0.2 V/s; [DOMA] = 1.45 mM.

the theoretical value of 30 mV for an electrochemically reversible two-electron process, the result is understandable if the rate constants for heterogeneous electron transfer, $k_{f,h}$ and $k_{b,h}$, are small [13]. Evidence consistent with this interpretation includes: (1) the peak potential separation for the chemically reversible oxidation of DOMA increases with increasing scan rate and (2) the peak potential separation for catechol, which is known to be oxidized reversibly to *o*-benzoquinone, is approximately 1.15 V when $v = 100$ V/s and pH = 2 (data not shown).

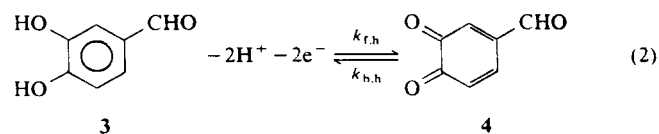
The number of electrons involved in the initial oxidation of DOMA was ascertained from single potential step chronoamperometric measurements. In this experiment, the potential is stepped anodically from a value ($E = 0.0$ V) where oxidation of DOMA is unaffected, to a sufficiently positive value ($E = 1.35$ V) such that the concentration of DOMA at the electrode surface is effectively zero. By comparison of the resulting diffusion-controlled chronoamperometric $it^{1/2}$ value for the oxidation of DOMA at $g \leq 100$ ms with that for the diffusion-controlled, two-electron oxidation of catechol and assuming that the diffusion coefficients of DOMA and catechol are similar, the n value for the initial oxidation of DOMA was determined to be 2 (Eqn. 1).



Evidence that the electrochemical oxidation of DOMA affords the *o*-benzoquinone **2** rather than the corresponding *p*-benzoquinone methide will be presented below.

Examination of Fig. 1a and b will show the presence of a second cathodic peak at a potential that is positive with respect to that for the reduction of **2**. The relative magnitude of this peak is kinetically controlled and increases with decreasing scan rate. In addition, when the scan rate is only 0.2 V/s (Fig. 1b), the potential for the anodic peak for the oxidation of DOMA is approx. 0.2 V more negative on the second cycle than on the first cycle. From cyclic voltammetric and HPLC studies of the products that are formed in the controlled-potential electrolysis of DOMA (*vide infra*), we ascertained that the appearance of the more positive cathodic peak and the negative shift in the anodic peak potential from the first to the second cycle is due to the decomposition of **2** and the formation of DOBAL (**3**). DOBAL is oxidized reversibly at the potential of the second cycle's

anodic peak to its corresponding *o*-benzoquinone, **4** (Eqn. 2). The latter species is then reduced at the



potential of the more positive cathodic peak on the reverse, negative-going half cycle.

The appearance of a single anodic peak for the oxidation of DOMA in the presence of electrogenerated DOBAL is understandable as long as 4-formyl-1,2-benzoquinone is thermodynamically and kinetically capable of oxidizing DOMA under these reaction conditions. Because we expect the -CHO functional group of DOBAL to be more electron-withdrawing than the -CHOHCOOH moiety of DOMA, the equilibrium constant for the reaction that is described by Eqn. 3



should exceed unity. The fact that the cyclic voltammetric oxidation of DOBAL occurs more readily than that of DOMA is attributed to the former species having a larger heterogeneous rate constant for electrochemical oxidation. The smaller anodic-cathodic peak potential separation for the DOBAL/**4** redox couple (Fig. 2a) than for the DOMA/**2** redox couple (Fig. 1a) is consistent with this interpretation.

Although the DOBAL/**4** redox couple is chemically reversible at scan rates in excess of 10 V/s at pH 2, a second cathodic peak is readily discernible in the cyclic

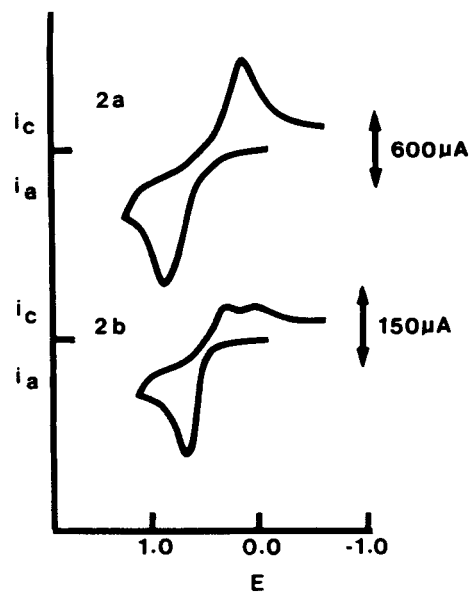
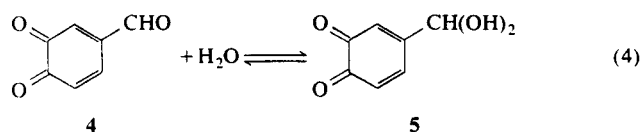


Fig. 2. Cyclic voltammograms of DOBAL on a carbon paste electrode surface at pH 2 and 23°C. (a) Scan rate 8 V/s; [DOBAL] = 1.1 mM. (b) Scan rate = 0.5 V/s; [DOBAL] = 1.1 mM.

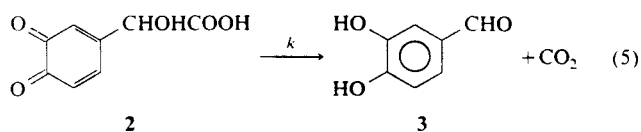
voltammograms of DOBAL at scan rates less than 2 V.s (Fig. 2b). We attribute the kinetically controlled behavior for the reduction of **4** and the appearance of a new cathodic peak at more negative potential to the hydration of **4** (Eqn. 4). Apparently, the aldehyde carbon of **4**



is substantially more electrophilic than the ring carbons. The more negative of the two cathodic peaks is assigned to the hydrated species (**5**) and occurs, as might be expected, at nearly the same potential as that for the reduction of **2** (Eqn. 1). Evidence consistent with this interpretation includes: (1) when DOBAL is partially oxidized at pH 2 by controlled potential electrolysis to **4** and **4** is subsequently reduced, product analysis by HPLC showed that only DOBAL was present; (2) electrochemical oxidation of 3,4-dihydroxybenzoic acid, which is incapable of undergoing the hydration reaction, did not afford a similar follow-up chemical reaction under these reaction conditions; and (3) the electrochemical oxidation of DOBAL is a diffusion-controlled, two-electron oxidation for $t \leq 10$ s (Buller, C.K.; Hawley, M.D., unpublished data). The last result precludes the formation of a reaction product that is oxidizable at the applied potential and eliminates, for example, a Michael addition of a nucleophile to the aromatic ring as a possible reaction pathway.

Kinetics of the oxidative decarboxylation reaction

The electrochemical oxidation of DOMA, the chemical transformation of **2** into DOBAL (Eqn. 5), and the



subsequent two-electron oxidation of DOBAL at the applied potential are an example of an ECE process; that is, a homogeneous chemical reaction (Eqn. 5) is interposed between electron transfer reactions (Eqn. 1 and 2) [14,15]. The electrochemical technique that was used to determine the rate constant for the transformation of **2** into DOBAL was single potential step chronoamperometry. The experiment was performed by stepping the potential from a value where neither oxidation nor reduction of DOMA occurs to a potential sufficiently positive such that the concentrations of DOMA and DOBAL at the electrode surface are effectively zero. The variation in $it^{1/2}$, which is proportional to the n value, is then observed as a function of $\log t$. For small values of the dimensionless parameter kt ,

where k is the first order rate constant and t is the elapsed time, the chemical reaction to produce additional electroactive species will not occur to any significant extent and a lower limit of 2 will be obtained for the n value. On the other hand, for large values of kt , all reactions will go to completion, thereby causing n to attain an upper limiting value of 4. For intermediate values of kt , the n value will increase smoothly from 2 to 4 with increasing t . The rate constant is obtained by fitting the experimental n value vs. $\log t$ curve to a dimensionless working curve of n vs. $\log kt$. A dimensionless working curve is obtained for each value K in Eqn. 3 by digital simulation of the processes described by Eqn. 1–3 and 5 [14].

Separate control experiments were performed to demonstrate that the chronoamperometric oxidation of 3,4-dihydroxybenzaldehyde was a diffusion-controlled, two-electron, oxidation process in the range $1 \leq \text{pH} \leq 6$ for $t \leq 10$ s. Thus, even though the controlled potential electrolysis data below suggest that 4-formyl-1,2-benzoquinone (or its corresponding hydrate) is unstable and affords additional electroactive products on the coulometric time scale, such a reaction is slow on the chronoamperometric time scale and does not affect the kinetic measurements of the homogeneous chemical reaction (Eqn. 5).

Typical results for the chronoamperometric oxidation of DOMA at pH 6 are shown in Fig. 3. The solid curve represents the theoretical variation of n with $\log t$ when the rate constant for the transformation of the DOMA oxidation product into DOBAL is 1.6 s^{-1} . The best fits of the experimental data with the theoretical working curve were obtained when the value of the equilibrium constant for the solution redox reaction was either unity ($\text{pH} \leq 2$) or $k_f/k_b = 0/0$ ($\text{pH} > 2$). The former result suggests that **4** may be present in solution largely in its hydrated form, **5**. If so, then the homoge-

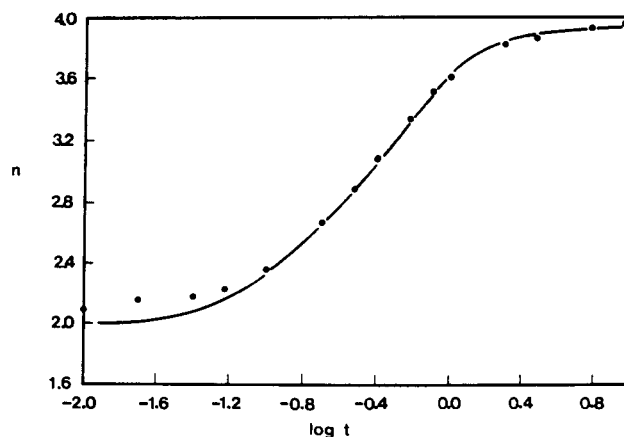
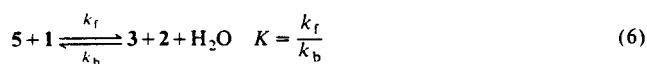


Fig. 3. Chronoamperometric results for the oxidation of 3.4 mM DOMA at pH 6. This solid curve represents the theoretical curve for an ECE mechanism in which $k = 1.6 \text{ s}^{-1}$ and $K = k_f/k_b = 0/0$ for the solution redox reaction (see text).

neous redox reaction would be described by Eqn. 6 rather than by Eqn. 3.



The fact that the reductions of **2** and **5** occur at nearly the same potential under similar conditions of scan rate and pH (compare Fig. 1b and 2b) is consistent with this interpretation. However, the best fit of the experimental data with the theoretical working curve for $K = k_f/k_b = 0/0$ implies that the solution redox reaction is not occurring above pH 2 on the time scale of the chronoamperometric experiment. This behavior is consistent with the observation that the peak potential for the oxidation of DOMA does not shift negatively from the first to the second cycle at pH 6 and also with the relatively small values of the heterogeneous electron transfer rate constants for the 1/2 and 3/4 redox complex throughout the pH range.

At any given value of pH in the range from 1 to 8, the chronoamperometric rate constant for the appearance of DOBAL was independent of the concentration of DOMA ($0.5 \text{ mM} \leq C \leq 4 \text{ mM}$). This result requires the rate-determining chemical reaction that transforms **2** into DOBAL (Eqn. 5) to be first-order with respect to DOMA [14,15]. In addition, the increase in the rate constant of the homogeneous chemical reaction over this same pH range ($0.2 \pm 0.3 \text{ s}^{-1}$ at pH 1, $0.3 \pm 0.2 \text{ s}^{-1}$ at pH 2, $0.8 \pm 0.3 \text{ s}^{-1}$ at pH 4, $1.6 \pm 0.2 \text{ s}^{-1}$ at pH 6 and $2.8 \pm 0.2 \text{ s}^{-1}$ at pH 8) is small (approx. 10-fold), which suggests that reaction 5 is not subject to acid or base catalysis. After this work had been completed, a rate constant of 2.8 s^{-1} at pH 6.3 was obtained for the decarboxylation of **2** by a pulse radiolysis method [11].

Coulometric data for the oxidation of DOMA

The product distribution as a function of the n value during the controlled-potential electrolysis of DOMA was monitored by HPLC and cyclic voltammetry. At pH 6 and an applied potential of 1.25 V, the concentration of DOMA decreased linearly to zero as the n -value increased linearly from zero to 2. DOBAL, which was the only significant product detected as long as $n \leq 2$, reached its maximum yield of 60% at $n = 2$; its yield then decreased linearly to zero as n increased from 2 to 5. These results suggest that, even though DOBAL is oxidized more readily than DOMA electrochemically, the oxidation of DOMA by **4** and **5** products (Eqn. 3 and 6), which is expected to be thermodynamically favorable, must be occurring in bulk solution on the coulometric time scale. Thus, as long as unreacted DOMA is present in bulk solution, there is no net oxidation of DOBAL. This behavior has facilitated the development of an assay that uses the production of

DOBAL from DOMA for the quantitation of diphenol oxidase activity [16]. Our data indicate that this assay will be valid as long as DOMA is present in excess. Although not all of the products that were detected by cyclic voltammetry and HPLC during prolonged electrolysis ($n \geq 2$) of DOMA were identified, species with the same electrochemical and chromatographic properties as standard compounds were formed during the controlled potential electrolysis of DOBAL (*vide infra*).

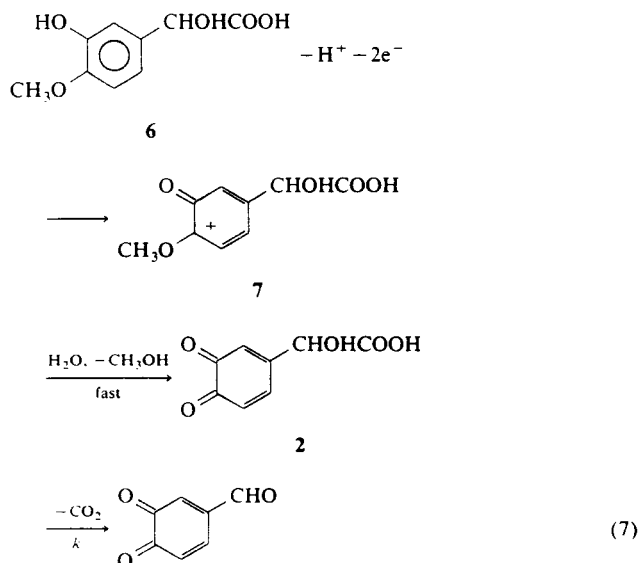
Coulometric data for the oxidation of DOBAL

The oxidation of DOBAL was shown above to be a diffusion-controlled, two-electron process on the chronoamperometric time scale ($t \leq 10 \text{ s}$). However, on the coulometric time scale, the initial products of DOBAL oxidation, **4** and its corresponding hydrate, **5**, were unstable at pH 6 and reacted to give additional electroactive products. When the total anodic peak current for the oxidation of DOBAL and its electrolysis products was plotted as a function of the n value, a straight line with an intercept of $n = 4$ was obtained (data not shown). Because the oxidation of **3** to **4** is nominally a two-electron process, this result implies that **4** must undergo some type of follow-up reaction to generate an electroactive species. No attempt was made to identify the follow-up reaction(s) or all of the products that were formed.

Redox behavior of mandelic acid-related compounds

In order to ascertain whether it is **2** or the corresponding *p*-benzoquinone methide that is formed as the initial product of the electrochemical oxidation of DOMA, the redox behaviors of several mandelic acid derivatives that would be expected to afford either the corresponding *p*-benzoquinone methide or the corresponding *o*-benzoquinone upon oxidation were examined. In all instances, severe electrode fouling occurred rapidly when compounds that were expected to give the corresponding *p*-benzoquinone methide as the intermediate were oxidized (e.g., 4-hydroxymandelic acid and 3-methoxy-4-hydroxymandelic acid). In contrast, 3-hydroxy-4-methoxymandelic acid (**6**) afforded essentially the same redox behavior as DOMA; i.e., and ECE reaction mechanism with the same first-order rate constant for the chemical appearance of DOBAL. These results require the initial oxidation product (**7**) of **6** to undergo rapid loss of methanol and to give the same intermediate (**2**) that undergoes the decarboxylation reaction (Eqn. 7). The ready loss of the methoxy moiety and the formation of the corresponding *o*-benzoquinone have been reported previously to occur in aqueous media upon electrochemical oxidation of *o*-methoxyphenol [17]. It is important to note that severe electrode fouling resulted only when direct formation of the corresponding *p*-benzoquinone methide was required or expected to occur. Because electrode fouling was not

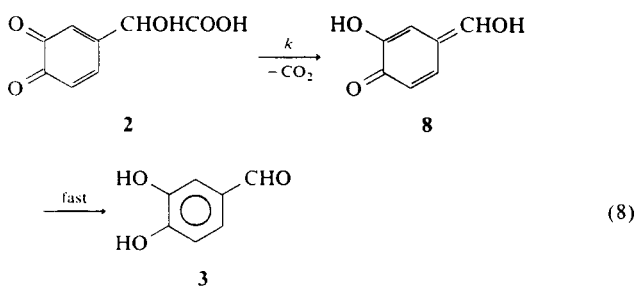
observed with DOMA or any other compound that was expected to give an *o*-benzoquinone as the oxidation product, we conclude that the *p*-benzoquinone methide



of DOMA is unlikely to be formed as a result of either the direct electrochemical oxidation of DOMA or the isomerization of *o*-benzoquinone 2.

Reaction pathway

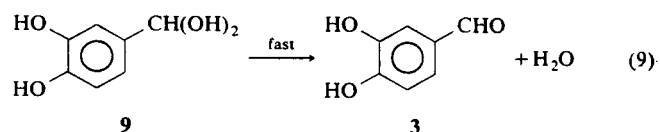
The results of the studies of the redox behavior of the several substituted mandelic acids are consistent with a pathway in which the oxidation of DOMA is initially a two-electron process that affords the corresponding *o*-benzoquinone, 2 (Eqn. 1). This species is unstable on the cyclic voltammetric time scale and undergoes decarboxylation to give the *p*-benzoquinone methide of 3,4-dihydroxybenzyl alcohol, 8, as a probable transient intermediate (Eqn. 8). The first-order kinetics for the



appearance of DOBAL could support either decarboxylation or isomerization of 8 to DOBAL as the rate-determining step. Although our results do not allow us to distinguish experimentally between these possibilities, no cyclic voltammetric peaks were observed in the cyclic voltammograms of DOMA that are unidentified and can be assigned to 8. Because the isomerization of 8 is expected to be rapid, loss of CO₂ from the *o*-benzo-

quinone of DOMA is favored as the rate-determining step.

Because the heterogeneous electron transfer rate constant for the oxidation of DOBAL is larger than that for DOMA, DOBAL is oxidized concomitantly with DOMA. The negative shift in the cyclic voltammetric anodic peak potential for the oxidation of DOMA that occurs between the first and second cycles is the result of the homogeneous oxidation of unreacted DOMA by electrogenerated 4 (Eqn. 3). However, once the concentration of DOMA has been depleted in the vicinity of the electrode surface, reactions described by Eqn. 4 and 6 can be expected to become increasingly important. At pH 2, the pseudo-first-order rate constant for the hydration of 4 is approximately twice as large as the rate constant for the decarboxylation of 2 (Buller, C.K.; Hawley, M.D., unpublished data). As evidenced by the presence of only one anodic peak in the cyclic voltammogram of DOBAL (Fig. 2b), the product 9 that arises from the two-electron reduction of 5 must rapidly lose water to regenerate DOBAL (Eqn. 9). Otherwise, 9



would be expected to afford an anodic peak at approximately the same potential as DOMA on the second and all subsequent cycles. The best fits of the chronoamperometric kinetic data for pH ≤ 2 were obtained for a value of $K = 1$ for the homogeneous redox reaction, which is in agreement with the observation that 2 and 5 are reduced at nearly the same potential. We do not have an explanation for the relatively small variation of the first-order rate constant with pH for the transformation of 2 into DOBAL and CO₂. Because the loss of a proton from the carboxylic acid moiety of 2 would be expected to proceed or be concerted with the elimination of CO₂, base catalysis had been anticipated to be important for pH ≤ pK_a. Although the pK_a of 2 is unknown, it is not unreasonable to expect this value to be approx. 4.

Concluding remarks

Several pathways have been proposed in the literature to account for the formation of DOBAL upon oxidation of DOMA. One involves decarboxylation of the initially formed DOMA-*o*-benzoquinone 2 to give the *p*-benzoquinone methide of 3,4-dihydroxybenzyl alcohol (8) as a transient intermediate; rearrangement of this species affords DOBAL [9,11,12]. A second pathway invokes a charge-transfer complex between DOMA and 2, with the former being oxidized and decarboxylated while the latter is simultaneously reduced to DOMA [10]. In a third pathway, the enzymatic oxida-

tion of DOMA by mushroom tyrosinase has been reported to yield directly the corresponding *p*-benzoquinone methide, from which decarboxylation occurs [7,8]. Our data support the first pathway; that is, the direct formation of the conventional *o*-benzoquinone **2**, followed by the rate-determining decarboxylation of **2** and the formation of the *p*-benzoquinone methide of 3,4-dihydroxybenzyl alcohol (**8**) as a transient, unobserved intermediate. Moreover, our data show that the product that arises from the rearrangement of **8**, 3,4-dihydroxybenzaldehyde (**3**), is also electroactive and that its oxidation product, 4-formyl-1,2-benzoquinone (**4**), undergoes relatively rapid hydration under these reaction conditions. Because both **4** and the hydrated species **5** may also oxidize unreacted DOMA (**1**), the electrochemical oxidative decarboxylation of DOMA is a reasonably complicated process.

p-Benzoquinone methides have been proposed as transient intermediates in a number of oxidation pathways, but there are only a few examples where a relatively reactive *p*-benzoquinone methide has been unambiguously identified [18]. Our group and others [9–11] have provided circumstantial evidence for the intermediacy of *p*-benzoquinone methide **8** in the formation of **3** from **1**. The results of our kinetic studies provide a maximum limit of a few tenths of a second for $t_{1/2}$ for **8** if the rate-determining step is rearrangement of **8** to **3**. On the other hand, if the loss of CO₂ from **2** is the rate-determining step, as we suspect, then the lifetime of **8** should be considerably shorter. In view of the consistency of data from several laboratories (Refs. 9–11, this study) and the experimental difficulty that would be required to observe **8** directly, we did not feel that an attempt to examine **8** directly could be justified at this time.

Acknowledgements

Contribution number 91-15-J from the Kansas Agricultural Experiment Station, Manhattan, KS. Cooper-

ative investigation between KAES and ARS-USDA. We gratefully acknowledge the partial support of this work by National Science Foundation grants CHE-8714657 and DCB-8609717.

References

- 1 Brunet, P.C.J. (1980) *Insect Biochem.* 10, 467–500.
- 2 Lerch, K. (1981) *Met. Ions Biol. Syst.* 13, 143–186.
- 3 Robb, R. (1984) in *Copper Proteins and Copper Enzymes* (Lonti, R., ed.), pp. 207–241, CRC Press, Boca Raton.
- 4 Toussaint, O. and Lerch, K. (1987) *Biochem.* 26, 8567–8571.
- 5 Atkinson, P.W. and Brown, W.V.; Gilby, A.R. (1973) *Insect. Biochem.* 3, 309–315.
- 6 Lake, C.R., Mills, R.R. and Koeppel, J.K. (1975) *Insect. Biochem.* 5, 223–229.
- 7 Sugumaran, M. (1986) *Biochem.* 25, 4489–4492.
- 8 Sugumaran, M., Semensi, V., Dali, H. and Mitchell, W. (1989) *Biorg. Chem.* 17, 86–95.
- 9 Cabanes, J., Sanchez-Ferrer, A., Bru, R. and Garcia-Carmona, F. (1988) *Biochem. J.* 256, 681–684.
- 10 Ortiz, F.M., Serrano, J.T., Lopez, J.N.R., Castellanos, R.V., Teruel, J.A.L. and Garcia-Canovas, F. (1988) *Biochim. Biophys. Acta* 957, 158–163.
- 11 Bouheroum, M., Bruce, J.M. and Land, E.J. (1989) *Biochim. Biophys. Acta* 998, 57–62.
- 12 Presented at the 198th National Meeting of the American Chemical Society, Miami Beach, September, 1989; Abstract Number 24.
- 13 Bard, A.J. and Faulkner, L.R. (1980) *Electrochemical Methods*, Chapter 6, John Wiley & Sons, New York.
- 14 Hawley, M.D. and Feldberg, S.W. (1966) *J. Phys. Chem.* 70, 3459–3464.
- 15 Hawley, M.D., Tatawawadi, S.V., Piekarski, S. and Adams, R.N. (1967) *J. Am. Chem. Soc.* 89, 447–450.
- 16 Li, J., Christensen, B.M. and Tracy, J.W. (1990) *Analyt. Biochem.* 190, 354–359.
- 17 Hawley, M.D. and Adams, R.N. (1964) *J. Electroanal. Chem.* 8, 163–166.
- 18 Angle, S.R. and Turnbull, K.D. (1989) *J. Am. Chem. Soc.* 111, 1136–1138.